roles are also synergistic because the binding of CPX by its central helix strategically positions the accessory helix for clamping. The central helix binds to residues in both the v- and t-SNARE motifs present in the central and membrane-distal portions of the SNARE bundle (*9*, *10*), ensuring that CPX can only begin to interfere with SNARE assembly after the SNAREpin has zippered at least halfway. The accessory helix then binds weakly and therefore reversibly to sequences in the membrane-proximal portion of the t-SNARE, ideal for a toggle switch.

We present a highly constrained but still speculative molecular model (Fig. 4) for the clamped state [details are in (*24*)] that establishes the structural feasibility of the proposed clamped state. The displaced sequences of VAMP2 include both the cleavage site and the protein recognition sequence for cleavage of VAMP2 by BoNTB toxin, which can still act on VAMP2 in the clamped state (*4*, *12*), but the recognition sequence for tetanus toxin is assembled into the four-helix bundle in the model, explaining why the CPX-clamped intermediate was found to be resistant to this toxin. We note that, in addition to its role as clamp, CPX is also positively required for fusion in an earlier step that requires the central helix and the N-terminal domain of 26 residues, but not the accessory helix (*19*). Ultimately, high-resolution structural studies will be needed to confirm the general outline of this model and provide intimate details, although the need for membrane insertion currently prevents this, necessitating less direct but, we believe, still forceful alternative approaches to central mechanistic problems in the control of membrane fusion.

References and Notes

1. T. Sollner *et al.*, *Nature* **362**, 318 (1993).
2. T. Weber *et al.*, *Cell* **92**, 759 (1998).
3. F. Li *et al.*, *Nat. Struct. Mol. Biol.* **14**, 890 (2007).
4. S. Y. Hua, M. P. Charlton, *Nat. Neurosci.* **2**, 1078 (1999).
5. S. M. Wojcik, N. Brose, *Neuron* **55**, 11 (2007).
6. T. W. Koh, H. J. Bellen, *Trends Neurosci.* **26**, 413 (2003).
7. T. C. Sudhof, *Annu. Rev. Neurosci.* **27**, 509 (2004).
8. J. Tang *et al.*, *Cell* **126**, 1175 (2006).
9. X. Chen *et al.*, *Neuron* **33**, 397 (2002).
10. A. Bracher, J. Kadlec, H. Betz, W. Weissenhorn, *J. Biol. Chem.* **277**, 26517 (2002).
11. S. Pabst *et al.*, *J. Biol. Chem.* **275**, 19808 (2000).
12. C. G. Giraudo, W. S. Eng, T. J. Melia, J. E. Rothman, *Science* **313**, 676 (2006); published online 22 June 2006 (10.1126/science.1129450).
13. T. C. Sudhof, *Nature* **375**, 645 (1995).
14. M. Geppert *et al.*, *Cell* **79**, 717 (1994).
15. C. Li *et al.*, *Nature* **375**, 594 (1995).
16. R. B. Sutton, D. Fasshauer, R. Jahn, A. T. Brunger, *Nature* **395**, 347 (1998).
17. M. Xue *et al.*, *Nat. Struct. Mol. Biol.* **14**, 949 (2007).
18. C. G. Giraudo *et al.*, *J. Biol. Chem.* **283**, 21211 (2008).
19. A. Maximov, J. Tang, X. Yang, Z. P. Pang, T. C. Südhof, *Science* **323**, 516 (2009).
20. Single-letter abbreviations for the amino acid residues are as follows: A, Ala; C, Cys; D, Asp; E, Glu; F, Phe; G, Gly; H, His; I, Ile; K, Lys; L, Leu; M, Met; N, Asn; P, Pro; Q, Gln; R, Arg; S, Ser; T, Thr; V, Val; W, Trp; and Y, Tyr.
21. C. Hu *et al.*, *Science* **300**, 1745 (2003).
22. T. J. Melia *et al.*, *J. Cell Biol.* **158**, 929 (2002).
23. C. G. Giraudo *et al.*, *J. Cell Biol.* **170**, 249 (2005).
24. Materials and methods are available as supporting material on *Science* Online.
25. A. Jones, O, version 12.0 (2008), http://xray.bm.nu.se/~alwyn/index.html

26. This work was supported by an NIH grant to J.E.R.

Supporting Online Material

www.sciencemag.org/cgi/content/full/323/5913/512/DC1
Materials and Methods
Figs. S1 to S3
References

29 September 2008; accepted 5 December 2008
10.1126/science.1166500

Complexin Controls the Force Transfer from SNARE Complexes to Membranes in Fusion

Anton Maximov,[1]* Jiong Tang,[1]† Xiaofei Yang,[1,2] Zhiping P. Pang,[1,2] Thomas C. Südhof[1,2,3,4,5]‡

Trans–SNAP receptor (SNARE, where SNAP is defined as soluble NSF attachment protein, and NSF is defined as *N*-ethylmaleimide–sensitive factor) complexes catalyze synaptic vesicle fusion and bind complexin, but the function of complexin binding to SNARE complexes remains unclear. Here we show that in neuronal synapses, complexin simultaneously suppressed spontaneous fusion and activated fast calcium ion–evoked fusion. The dual function of complexin required SNARE binding and also involved distinct amino-terminal sequences of complexin that localize to the point where trans-SNARE complexes insert into the fusing membranes, suggesting that complexin controls the force that trans-SNARE complexes apply onto the fusing membranes. Consistent with this hypothesis, a mutation in the membrane insertion sequence of the v-SNARE synaptobrevin/vesicle-associated membrane protein (VAMP) phenocopied the complexin loss-of-function state without impairing complexin binding to SNARE complexes. Thus, complexin probably activates and clamps the force transfer from assembled trans-SNARE complexes onto fusing membranes.

Synaptic vesicle fusion is driven by assembly of trans–SNAP receptor (SNARE, where SNAP is defined as soluble NSF attachment protein, and NSF is defined as *N*-ethylmaleimide–sensitive factor) complexes (or SNAREpins) from syntaxin-1 and SNAP-25 on the plasma membrane and synaptobrevin/vesicle-associated membrane protein (VAMP) on the vesicle membrane (*1*–*3*). Ca^{2+} then triggers fast synchronous synaptic vesicle fusion by binding to the Ca^{2+}-sensor synaptotagmin (*4*–*6*). Besides SNARE proteins and synaptotagmin, fast Ca^{2+}-triggered fusion requires complexin (*7*). Complexin is composed of short N- and C-terminal sequences and two central α helices. Complexin binds to SNARE complexes via its central α helix, which inserts in an antiparallel orientation into a groove formed by synaptobrevin/VAMP and syntaxin-1 (*8*, *9*). Although multiple approaches have revealed an essential role of complexin in synaptic fusion (*7*, *10*–*15*), the nature of this role remains unclear. In vertebrate autapses, the deletion of complexin selectively impairs fast synchronous neurotransmitter release without changing asynchronous or spontaneous release (*7*, *10*). Conversely, in in vitro fusion assays, the addition of complexin causes a general block of SNARE-dependent fusion, indicating that complexin is a SNARE clamp (*11*–*14*). In *Drosophila* neuromuscular synapses, the deletion of complexin produces a >20-fold increase in spontaneous release but only a small decrease in evoked release (*15*). Thus, the role of complexin in fusion is unclear. Moreover, even the importance of complexin SNARE-complex binding remains uncertain (*16*, *17*). We addressed these questions with two complementary approaches: (i) RNA interference–mediated knockdown of complexin with rescue and (ii) replacing wild-type (WT) synaptobrevin with specific mutants using synaptobrevin knockout (KO) mice (*18*).

We knocked down complexin expression in cultured cortical neurons with the use of a short hairpin RNA (shRNA) that targets both complexin-1 and -2, the only complexin isoforms detectably expressed in these neurons (*19*). For this purpose, we used lentiviruses that simultaneously synthesize the complexin shRNA and either green fluorescent protein (GFP), WT complexin-1, or 4M-mutant complexin-1 that is unable to bind to SNARE complexes because it contains four amino acid substitutions [R48A/R59A/K69A/Y70A; for these substitutions and

[1]Department of Neuroscience, University of Texas Southwestern Medical Center, Dallas, TX 75390, USA. [2]Department of Cellular and Molecular Physiology, Stanford University, 1050 Arastradero Road, Palo Alto, CA 94304–5543, USA. [3]Department of Molecular Genetics, University of Texas Southwestern Medical Center, Dallas TX 75390, USA. [4]Howard Hughes Medical Institute, University of Texas Southwestern Medical Center, Dallas, TX 75390, USA. [5]Howard Hughes Medical Institute, Stanford University, Palo Alto, CA 94304–5543, USA.

*Present address: Department of Cell Biology, The Scripps Research Institute, La Jolla, CA 92037, USA.
†Present address: Stanford University, Stanford, CA 94305, USA.
‡To whom correspondence should be addressed. E-mail: tcs1@stanford.edu

the synaptobrevin substitutions described below, amino acids are written in single-letter code (*19*); for example, R48A signifies the arginine-to-alanine substitution at position 48] (*20*, *21*). Lentivirus expressing GFP without the shRNA served a further control. This design enabled us to simultaneously analyze control neurons and complexin knock-down neurons expressing either GFP, WT complexin (as a rescue control), or 4M-mutant complexin. The shRNA strongly inhibited the expression of complexin-1 and -2, whereas the expression of other proteins (including SNARE proteins) was unchanged, and synapse numbers were unaltered (figs. S1 and S2).

The complexin knockdown increased by three- to fourfold the frequency of spontaneous miniature excitatory postsynaptic currents (mEPSCs), without altering the mEPSC amplitude (Fig. 1A). In contrast, the complexin knockdown decreased by three- to fourfold the amplitude of EPSCs evoked by isolated action potentials (Fig. 1B). Evoked EPSCs could not be restored by increasing the extracellular Ca^{2+} concentration, identifying complexin as a central component of the Ca^{2+}-triggering machinery (fig. S3). Both changes were rescued by WT, but not by 4M-mutant, complexin, confirming the specificity of the shRNA and the importance of SNARE binding. Finally, the complexin knockdown decreased the initial EPSCs during a 10-Hz stimulus train but did not alter the total synaptic charge transfer evoked by the train and even increased the delayed EPSCs following the train (fig. S4). Thus, the complexin knockdown greatly impaired fast synchronous, but not asynchronous, synaptic vesicle fusion and increased spontaneous fusion, thereby reconciling the divergent phenotypes observed in vertebrate autapses, *Drosophila* neuromuscular junctions, and in vitro fusion assays (*7*, *10*–*15*).

We next examined which complexin sequences mediate spontaneous and evoked fusion (Fig. 1C). An N-terminal deletion of 40 residues ($Cpx^{41–134}$) abolished all complexin function (Fig. 1, D and E). This abolishment was not due to an impairment in SNARE-complex binding in competition with synaptotagmin, because a complexin fragment containing only its central α-helical SNARE-binding

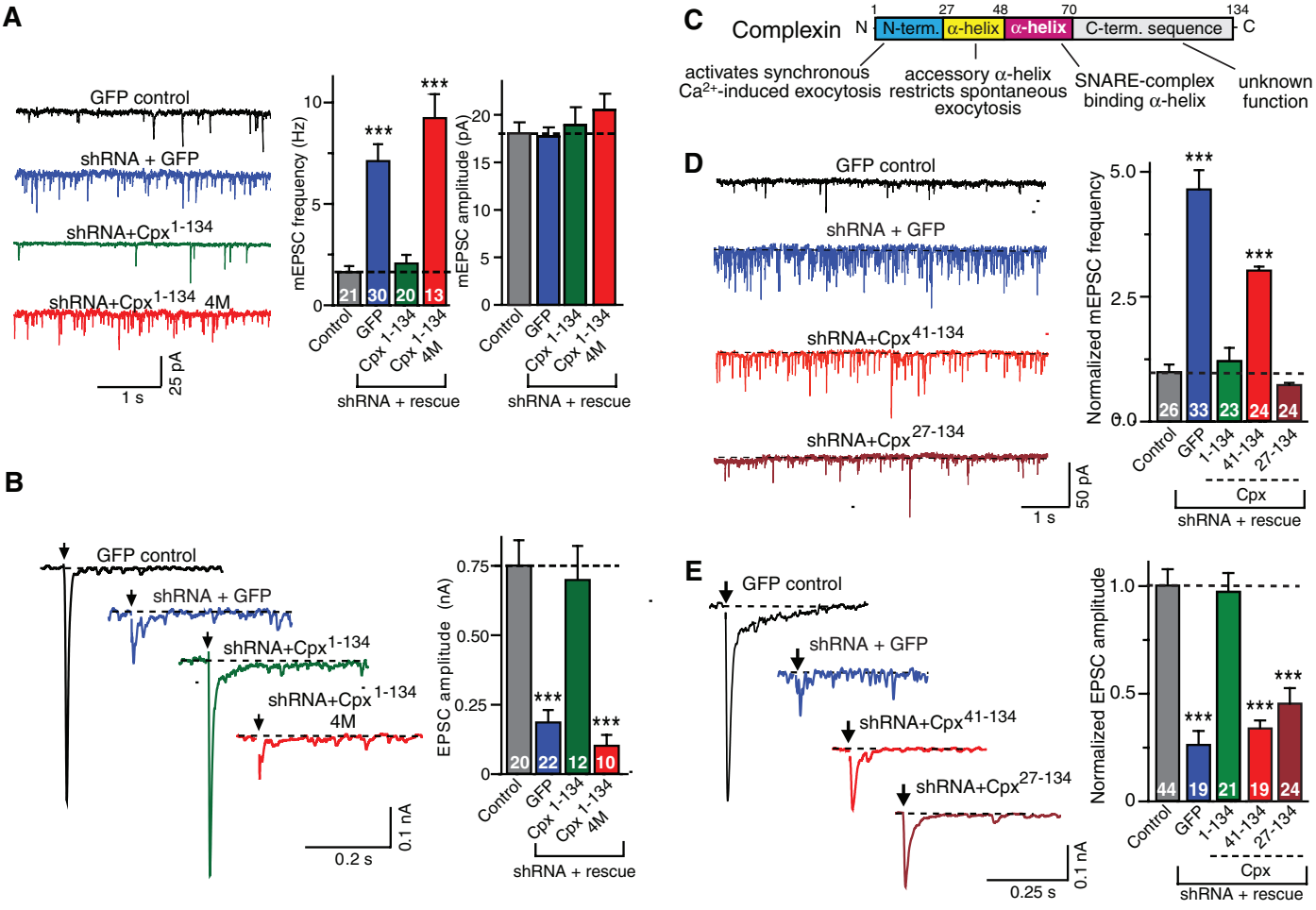

Fig. 1. Complexin knockdown increases spontaneous fusion but suppresses fast Ca^{2+}-evoked fusion. (**A**) Spontaneous fusion monitored as mEPSCs (left, representative traces; center and right, summary graphs of mEPSC frequencies and amplitudes, respectively). Recordings are from WT mouse neurons infected with lentiviruses expressing GFP only (control) or an shRNA that suppresses both complexin-1 and -2 and additionally expresses either GFP, WT rat complexin-1 ($Cpx^{1–134}$), or mutant rat complexin-1 with inactivated SNARE-binding sites ($Cpx^{1–134}$ 4M). For protein and synapse quantitations, see figs. S1 and S2; for calcium titrations of release, see fig. S3. (**B**) Ca^{2+}-evoked fusion monitored as EPSCs triggered by isolated action potentials at 0.1 Hz (left, representative traces; right, mean amplitudes). Neurons were infected with lentiviruses as described in (A). For responses elicited by 10-Hz stimulus trains, see fig. S4. (**C**) Domain structure of complexin and assignment of domains based on the rescue analysis shown in (D) and (E). (**D** and **E**) Complexin sequences required for rescue of the dual complexin loss-of-function phenotype: the increase in mEPSC frequency (D) and the decrease in EPSC amplitudes (E). Left, representative traces; right, summary graphs of mEPSC frequency (D) and EPSC amplitude (E), both normalized to control. Recordings were from mouse neurons infected with a lentiviruses expressing GFP only (control) or the complexin shRNA and either GFP or the indicated rat complexin-1 fragments. Scale bars apply to all traces in a group. Summary graphs depict means ± SEMs (see table S1 for numerical electrophysiology data). Statistical significance was evaluated by analysis of variance (ANOVA) in comparison to control neurons (triple asterisks denote $P < 0.001$); the total number of analyzed neurons in four to six independent cultures is shown in the bars.

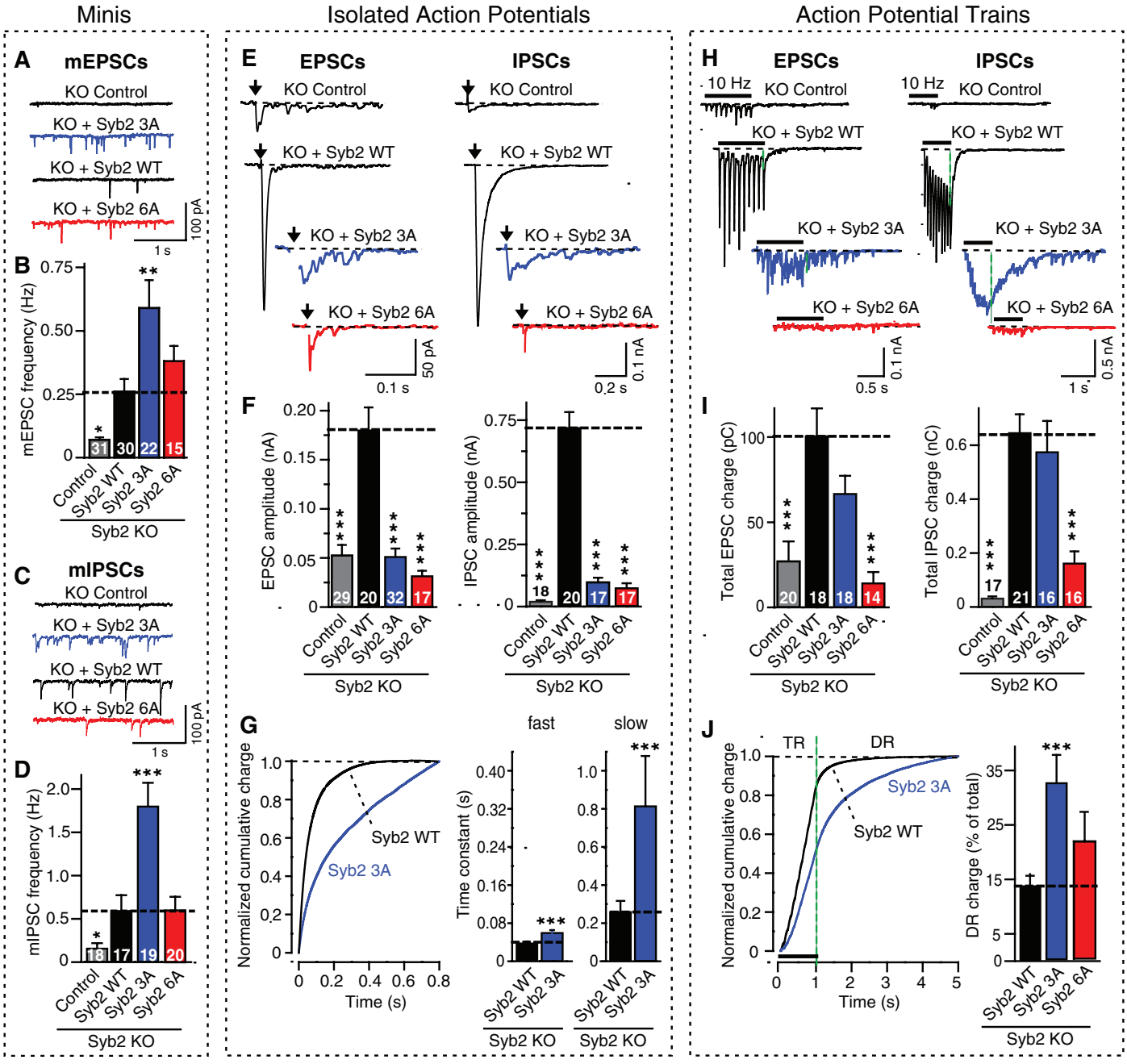

Fig. 2. Blocking complexin-binding to SNARE complexes increases spontaneous fusion but suppresses fast Ca^{2+}-evoked fusion. Synaptobrevin-2 KO neurons were infected with lentiviruses expressing GFP only (control) or WT (Syb2 WT), 3A-mutant (Syb2 3A), or 6A-mutant synaptobrevin-2 (Syb2 6A). The 3A-mutation in synaptobrevin selectively blocks complexin-binding to SNARE complexes, whereas the 6A-mutation additionally impairs SNARE-complex assembly (figs. S6 and S7). (**A** to **D**) Representative traces [(A) and (C)] and frequencies [(B) and (D)] of spontaneous mEPSCs [(A) and (B)] and miniature inhibitory postsynaptic currents (mIPSCs) [(C) and (D)]. For mini amplitudes, see fig. S8. (**E** and **F**) Representative traces (E) and mean amplitudes (F) of EPSCs (left) and IPSCs (right) evoked by isolated action potentials at 0.1 Hz. (**G**) Time course of isolated IPSCs monitored in synaptobrevin-2 KO neurons expressing WT (Syb2 WT) or 3A-mutant synaptobrevin-2 (Syb2 3A). The time course was analyzed as the cumulative normalized charge transfer (left) and fitted to a two-exponential equation yielding time constants of fast- and slow-release phases (right) (see fig. S9 illustrating scaled superimposed IPSC traces). (**H** and **I**) Representative traces (H) or mean synaptic charge transfer (I) of EPSCs (left) and IPSCs (right) evoked by 10-Hz action potential trains (see fig. S10 for quantitations of charge transfers). (**J**) Time course of the cumulative IPSC charge transfer during the 10-Hz stimulus train. (Left) Plots of the cumulative normalized charge transfer allow quantitation of train release (TR) and delayed release (DR; shown only for neurons expressing WT or 3A-mutant synaptobrevin-2). (Right) Bar diagram of the contribution of delayed release to the total synaptic charge transfer in neurons expressing WT (Syb2 WT), 3A-mutant (Syb2 3A), and 6A-mutant synaptobrevin-2 (Syb2 6A). All scale bars apply to all traces in a series, and all bar diagrams depict means ± SEMs. Statistical significance was evaluated by ANOVA in comparison to WT synaptobrevin-2: Single asterisks denote $P < 0.05$; double asterisks $P < 0.01$; and triple asterisks $P < 0.001$; the total number of analyzed neurons in five to six independent cultures is shown in the summary bars.

sequence ($Cpx^{41–86}$) still bound to SNARE complexes and potently inhibited synaptotagmin-binding to SNARE complexes (fig. S5). Thus, SNARE-complex binding in competition with synaptotagmin is necessary but not sufficient for complexin function, which also requires its N-terminal sequence. Additional dissection of this N-terminal sequence revealed that the nonstructured N-terminal complexin sequence is essential for activating fast fu-

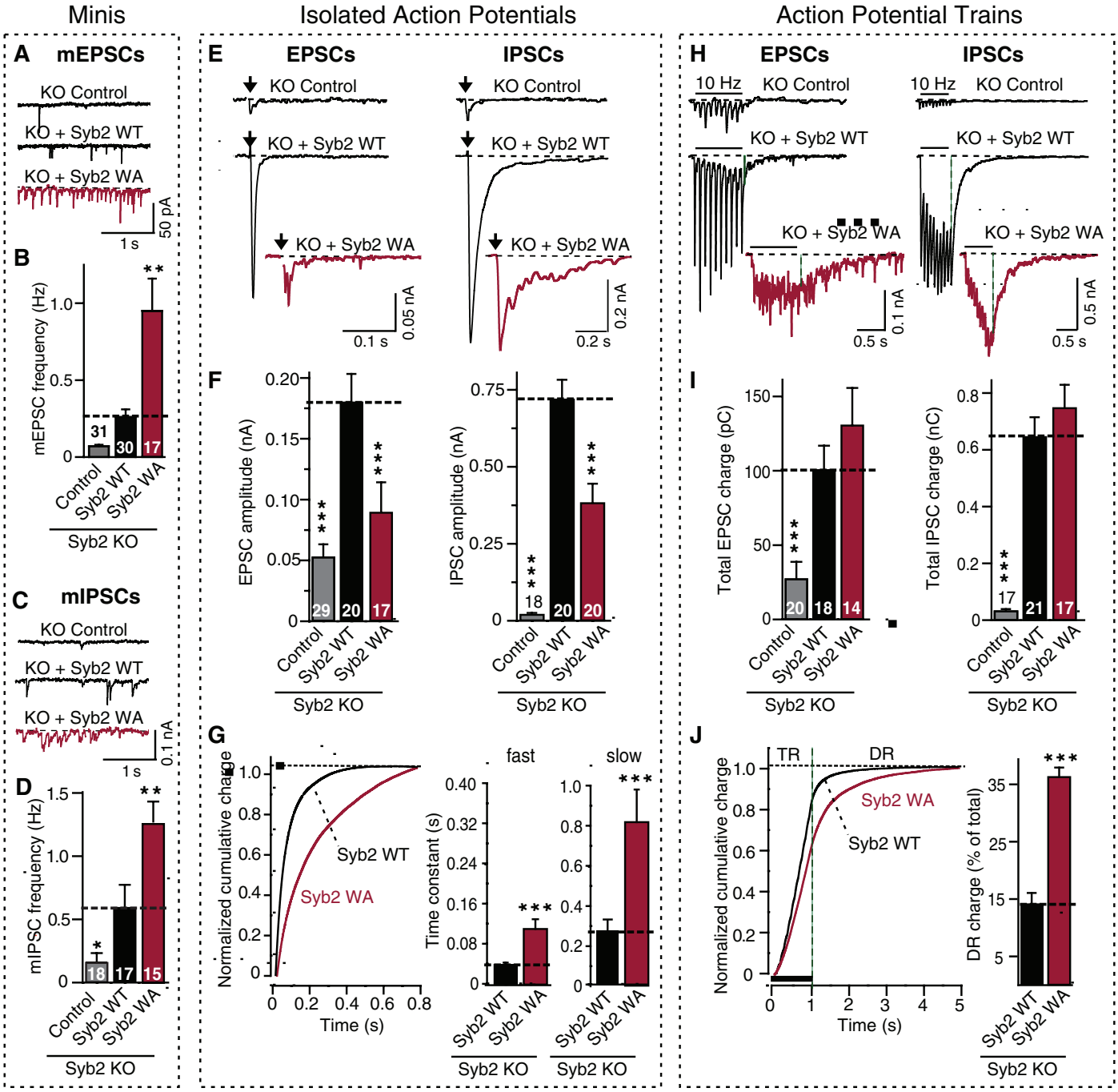

Fig. 3. A mutation in the membrane-insertion sequence of synaptobrevin (WA-mutation) phenocopies the complexin knockdown. Recordings were performed in synaptobrevin-2 KO neurons expressing either GFP only (control), WT (Syb2 WT), or WA-mutant (Syb2 WA; see figs. S6 and S7). (**A** to **D**) Representative traces [(A) and (C)] and mean frequencies [(B) and (D)] of spontaneous mEPSCs [(A) and (B)] and mIPSCs [(C) and (D)]. For synaptic targeting of WA-mutant synaptobrevin-2, see fig. S11; for mini amplitudes, see fig. S12. (**E** and **F**) Representative traces (E) and mean amplitudes (F) of EPSCs (left) and IPSCs (right) evoked by isolated action potentials at 0.1 Hz. (**G**) Time course of isolated IPSCs, analyzed as cumulative normalized charge transfer (left) and fitted to a two-exponential equation yielding time constants of fast and slow phases of release (right) (see fig. S9 for scaled superimposed IPSC traces). (**H** and **I**) Representative traces (H) and mean synaptic charge transfer (I) of EPSCs (left) and IPSCs (right) evoked by 10-Hz action potential trains (see. fig. S14 for quantitations of charge transfers). (**J**) Time course of the cumulative IPSC charge transfer during the 10-Hz stimulus train, analyzed as the cumulative normalized charge transfer and illustrated as the fraction of delayed release of the total synaptic charge transfer (right). All scale bars apply to all traces in a series, and all bar diagrams depict means ± SEMs. Statistical significance was evaluated by ANOVA in comparison to WT synaptobrevin-2: Single asterisks denote $P < 0.05$; double asterisks $P < 0.01$; and triple asterisks $P < 0.001$; the total number of analyzed neurons in five to six independent cultures is shown in the bars in (B), (D), (F), and (I).

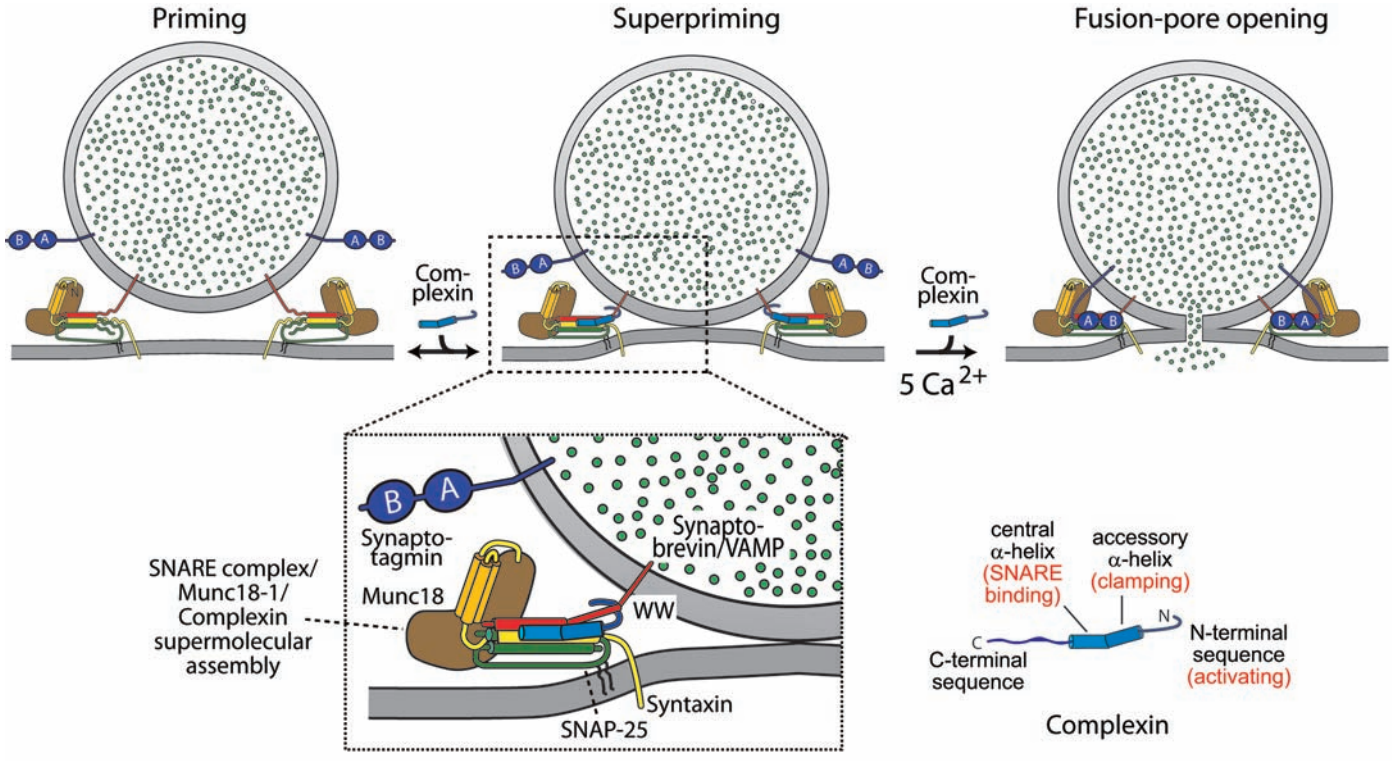

Fig. 4. Complexin action in SNARE-dependent fusion during fusion a vesicle goes through three stages: (i) priming, (ii) superpriming, and (iii) fusion pore opening (**top**). Complexin is proposed to suppress spontaneous fusion by inserting into the assembling trans-SNARE complex and to activate evoked fusion by directly or indirectly interacting with the membrane-insertion sequence of SNARE proteins in the trans-complex (**bottom**). Complexin binding to trans-SNARE complexes simultaneously stabilizes SNARE complex assembly, blocks completion of assembly, and inhibits the transfer of the force generated by SNARE-complex assembly onto the fusing membranes. Synaptotagmin subsequently triggers fusion by reversing the complexin block on activated SNARE complexes in addition to its Ca^{2+}-dependent phospholipid-binding activity (*21*). Note that the C-terminal complexin sequence is not shown in the fusion diagrams to simplify the presentation.

sion but not for clamping spontaneous fusion (Fig. 1, D and E), indicating distinct sequence requirements for the dual activating/clamping functions of complexin.

To further analyze complexin function, we used synaptobrevin-deficient neurons that lack both spontaneous and evoked synaptic fusion (*18*). Expression of WT synaptobrevin rescued the loss of fusion in synaptobrevin-deficient neurons. In contrast, 3A-mutant synaptobrevin that forms SNARE-complexes normally but cannot support complexin binding to these SNARE complexes (figs. S6 and S7) not only rescued spontaneous fusion but increased it more than twofold above WT levels (Fig. 2, A to D). At the same time, 3A-mutant synaptobrevin decreased evoked fusion and decelerated and desynchronized its time course (Fig. 2, E to G, and figs. S8 and S9). Moreover, although fusion elicited by a 10-Hz stimulus train was initially decreased in synapses expressing 3A-mutant synaptobrevin, fusion quickly recovered, such that the total synaptic charge transfer evoked by the stimulus train was normal, and the amount of delayed fusion after the stimulus train was enhanced (Fig. 2, H to J, and fig. S10). A second synaptobrevin mutation (the 6A-mutation) that impaired both SNARE-complex formation and complexin binding to SNARE complexes did not rescue the decrease in evoked release induced by either isolated action potentials or the stimulus train of action potentials (Fig. 2). Thus, the block of complexin binding by the 3A-mutation caused a selective loss of synchronous fast fusion, different from the impairment of all fusion caused by the inhibition of SNARE-complex assembly produced by the 6A-mutation.

The location of the N-terminal sequence of complexin at the point where SNARE complexes insert into the membrane suggests that the N-terminal complexin sequence may control the coupling of SNARE-complex assembly to membrane fusion. If so, complexin may act on SNARE sequences close to the membrane. We tested this hypothesis by mutating the juxta-membranous sequence of synaptobrevin/VAMP in three sets of alanine substitutions: K85A/R86A, R86A/K87A, and W89A/W90A, where W is Trp (referred to as the 85-, 86-, and WA-mutations, respectively) (figs. S6 and S7).

The WA-mutation had no effect on SNARE-complex stability, complexin- or synaptotagmin-binding to SNARE complexes, or synaptobrevin targeting to synapses (figs. S6, S7, and S11), but it caused a two- to threefold increase in mini frequency without a change in mini amplitude (Fig. 3, A to D, and fig. S12). Moreover, the WA-mutation produced an approximately twofold decrease in fast evoked fusion, with the remaining fusion being largely asynchronous because its kinetics were decelerated two- to threefold (fig. 3, E to G, and fig. S9). Again, as observed for complexin knockdown neurons and neurons expressing 3A-mutant synaptobrevin that lacked complexin binding, synaptic vesicle fusion induced by a 10-Hz stimulus train was only impaired during the initial synchronous responses. Later responses during the train's asynchronous phase were normal, and delayed release was enhanced (Fig. 3, H to J, and fig. S13), thus rendering the WA-mutation a weaker phenocopy of the synaptotagmin-1 KO, the complexin KO, the complexin knockdown, and the synaptobrevin 3A-mutation phenotype (*7*, *15*, *22*) (Figs. 1 to 3). In contrast to the WA-mutation, the 85- and 86-mutations did not impair rescue of synaptic transmission by synaptobrevin in synaptobrevin-deficient neurons (fig. S14), thus confirming the specificity of the WA-rescue phenotype.

Here, we have shown that in neuronal synapses, complexin acted both as a clamp and as an activator of SNAREs. These functions required complexin binding to SNARE-complexes and depended on distinct N-terminal complexin sequences that localize to the point where trans-SNARE complexes insert into the two fusing membranes. A mutation in the juxta-membranous sequence of synaptobrevin phenocopies the complexin loss-of-function phenotype. Thus, the simultaneous control of spontaneous and evoked fusion by complexin appears to involve the translation of

the force generated by assembly of trans-SNARE complexes onto the two fusing membranes (Fig. 4), consistent with biochemical data (*23*). We postulate that after complexin binds to assembling SNARE complexes, its N-terminal sequence activates and clamps the force generated by SNARE-complex assembly. The N terminus of complexin might perform its activator function by pulling the complex closer to the membrane, possibly by binding to phospholipids, whereas the accessory N-terminal α-helix might clamp the complex by inserting into the space between the v- and t-SNAREs or even substituting for one of the SNAREs in the C-terminal segment of the trans-SNARE complex (*24*). Once anchored on the SNARE complex, the 40 N-terminal residues of complexin both activate and clamp SNARE complexes to control fast Ca^{2+}-triggered neurotransmitter release in a process that is conserved in all animals. Viewed in the broader picture, complexin and synaptotagmin therefore operate as interdependent clamp-activators of SNARE-dependent fusion, with synaptotagmin exploiting the activator effect of complexin and reversing its clamping function (*11*, *21*, *22*). In this molecular pas-de-deux, the functions of both proteins are intimately linked: Their phenotypes are identical both as activators and as clamps, and one does not operate without the other.

References and Notes

1. J. B. Sørensen, *Trends Neurosci.* **28**, 453 (2005).
2. R. Jahn, R. H. Scheller, *Nat. Rev. Mol. Cell Biol.* **7**, 631 (2006).
3. M. Verhage, R. F. Toonen, *Curr. Opin. Cell Biol.* **19**, 402 (2007).
4. M. Geppert *et al.*, *Cell* **79**, 717 (1994).
5. R. Fernandez-Chacon *et al.*, *Nature* **410**, 41 (2001).
6. M. Yoshihara, J. T. Littleton, *Neuron* **36**, 897 (2002).
7. K. Reim *et al.*, *Cell* **104**, 71 (2001).
8. X. Chen *et al.*, *Neuron* **33**, 397 (2002).
9. A. Bracher, J. Kadlec, H. Betz, W. Weissenhorn, *J. Biol. Chem.* **277**, 26517 (2002).
10. M. Xue *et al.*, *Nat. Struct. Mol. Biol.* **14**, 949 (2007).
11. C. G. Giraudo, W. S. Eng, T. J. Melia, J. E. Rothman, *Science* **313**, 676 (2006), published online 22 June 2006; 10.1126/science.1129450.
12. C. G. Giraudo *et al.*, *J. Biol. Chem.* **283**, 21211 (2008).
13. J. R. Schaub, X. Lu, B. Doneske, Y. K. Shin, J. A. McNew, *Nat. Struct. Mol. Biol.* **13**, 748 (2006).
14. T. Y. Yoon *et al.*, *Nat. Struct. Mol. Biol.* **15**, 707 (2008).
15. S. Huntwork, J. T. Littleton, *Nat. Neurosci.* **10**, 1235 (2007).
16. K. Weninger, M. E. Bowen, U. B. Choi, S. Chu, A. T. Brunger, *Structure* **16**, 308 (2008).
17. R. Guan, H. Dai, J. Rizo, *Biochemistry* **47**, 1474 (2008).
18. S. Schoch *et al.*, *Science* **294**, 1117 (2001).
19. Single-letter abbreviations for the amino acid residues are as follows: A, Ala; C, Cys; D, Asp; E, Glu; F, Phe; G, Gly; H, His; I, Ile; K, Lys; L, Leu; M, Met; N, Asn; P, Pro; Q, Gln; R, Arg; S, Ser; T, Thr; V, Val; W, Trp; and Y, Tyr.
20. For a description of the experimental procedures, see the supporting online material.
21. J. Tang *et al.*, *Cell* **126**, 1175 (2006).
22. A. Maximov, T. C. Südhof, *Neuron* **48**, 547 (2005).
23. K. Hu, J. Carroll, C. Rickman, B. Davletov, *J. Biol. Chem.* **277**, 41652 (2002).
24. C. G. Giraudo *et al.*, *Science* **323**, 512 (2009).

25. We thank J. Rizo and L. Chen for advice and critical comments. This study was supported by an investigatorship to T.C.S. from the Howard Hughes Medical Institute.

Supporting Online Material

www.sciencemag.org/cgi/content/full/323/5913/516/DC1
SOM Text
Figs. S1 to S14
Table S1
References

29 September 2008; accepted 5 December 2008
10.1126/science.1166505

Widespread Increase of Tree Mortality Rates in the Western United States

Phillip J. van Mantgem,[1]*†‡ Nathan L. Stephenson,[1]*† John C. Byrne,[2] Lori D. Daniels,[3] Jerry F. Franklin,[4] Peter Z. Fulé,[5] Mark E. Harmon,[6] Andrew J. Larson,[4] Jeremy M. Smith,[7] Alan H. Taylor,[8] Thomas T. Veblen[7]

Persistent changes in tree mortality rates can alter forest structure, composition, and ecosystem services such as carbon sequestration. Our analyses of longitudinal data from unmanaged old forests in the western United States showed that background (noncatastrophic) mortality rates have increased rapidly in recent decades, with doubling periods ranging from 17 to 29 years among regions. Increases were also pervasive across elevations, tree sizes, dominant genera, and past fire histories. Forest density and basal area declined slightly, which suggests that increasing mortality was not caused by endogenous increases in competition. Because mortality increased in small trees, the overall increase in mortality rates cannot be attributed solely to aging of large trees. Regional warming and consequent increases in water deficits are likely contributors to the increases in tree mortality rates.

As key regulators of global hydrologic and carbon cycles, forests are capable of contributing substantial feedbacks to global changes (*1*). Such feedbacks may already be under way; for example, forest carbon storage may be responding to environmentally driven changes in global patterns of tree growth and forest productivity (*2*–*4*). Recent warming has been implicated as contributing to episodes of forest dieback (pulses of greatly elevated tree mortality), such as those mediated by bark beetle outbreaks in western North America (*5*, *6*). Yet little effort has gone toward determining whether environmental changes are contributing to chronic, long-term changes in tree demographic rates (mortality and recruitment). Changes in demographic rates, when compounded over time, can alter forest structure, composition, and function (*7*). For example, a persistent doubling of background mortality rate (such as from 1 to 2% $year^{-1}$) ultimately would cause a >50% reduction in average tree age in a forest, and hence a potential reduction in average tree size. Additionally, changing demographic rates could indicate forests approaching thresholds for abrupt dieback. Yet spatially extensive analyses of long-term changes in tree demographic rates have been limited to tropical forests, where mortality and recruitment rates both have increased over the past several decades, perhaps in response to rising atmospheric CO_2 concentrations, nutrient deposition, or other environmental changes (*2*, *8*). Comparably extensive analyses have not been conducted in temperate forests.

We sought to determine whether systematic changes in tree demographic rates have occurred recently in coniferous forests of the western United States, and if so, to identify possible causes of those changes. Although the western United States has witnessed recent episodes of forest dieback related to bark beetle outbreaks or combinations of drought and outbreaks (*5*, *6*), most forested land continues to support seemingly healthy forests that have not died back (*9*). To minimize transient dynamics associated with stand development and succession, we limited our analyses to data from repeated censuses in undisturbed forest stands more than 200 years old (*10*). Old forests contain trees of all ages and sizes (*11*, *12*), and any large, persistent changes in demographic rates over a short period (such as a few decades) are likely to be consequences of exogenous environmental changes (*2*, *13*). In contrast, in young forests rapid demographic changes can sometimes result largely from endogenous processes (such as self-thinning during stand development) (*14*), potentially obscuring environmentally driven changes.

[1]U.S. Geological Survey, Western Ecological Research Center, Three Rivers, CA 93271, USA. [2]USDA Forest Service, Rocky Mountain Research Station, Moscow, ID 83843, USA. [3]Department of Geography, University of British Columbia, Vancouver, British Columbia V6T IZ2, Canada. [4]College of Forest Resources, University of Washington, Seattle, WA 98195, USA. [5]School of Forestry and Ecological Restoration Institute, Northern Arizona University, Flagstaff, AZ 86011, USA. [6]Department of Forest Science, Oregon State University, Corvallis, OR 97331, USA. [7]Department of Geography, University of Colorado, Boulder, CO 80309, USA. [8]Department of Geography, Pennsylvania State University, University Park, PA 16802, USA.

*These authors contributed equally to this work.
†To whom correspondence should be addressed. E-mail: pvanmantgem@usgs.gov (P.J.V.); nstephenson@usgs.gov (N.L.S.)
‡Present address: U.S. Geological Survey, Western Ecological Research Center, Arcata, CA 95521, USA.